High energy physics and the very early universe with LISA

Carlo Ungarelli*
School of Computer Science and Mathematics, University of Portsmouth, Mercantile House, Hampshire Terrace, Portsmouth P01 2EG, United Kingdom
and Max Planck Institut für Gravitationsphysik, Albert Einstein Institut Am Mühlenberg 1, D-14476 Golm, Germany

Alberto Vecchio†
Max Planck Institut für Gravitationsphysik, Albert Einstein Institut Am Mühlenberg 1, D-14476 Golm, Germany
(Received 8 March 2000; published 23 February 2001)

Gravitational wave experiments will play a key role in the investigation of the frontiers of cosmology and the structure of fundamental fields at high energies by either setting stringent upper limits on or by detecting the primordial gravitational wave background produced in the early Universe. Here we discuss the impact of space-borne laser interferometric detectors operating in the low-frequency window $\sim 10^{-6}$–1 Hz; the aim of our analysis is to investigate whether a primordial background characterized by a fractional energy density $h_{100}^2\Omega \sim 10^{-16} - 10^{-15}$, which is consistent with the prediction of ''slow-roll'' inflationary models, might be detectable by the Laser Interferometer Space Antenna (LISA) or follow-up missions. In searching for stochastic backgrounds, the presently planned LISA mission suffers from the lack of two detectors with uncorrelated noise. We analyze the sensitivity improvements that could be achieved by cross-correlating the data streams from a pair of detectors of the LISA class; we show that this configuration is extremely compelling, leading to the detection of a stochastic background as weak as $h_{100}^2\Omega \simeq 5\times 10^{-14}$. However, such instrumental sensitivity cannot be fully exploited to measure the primordial component of the background, due to the overwhelming power of the signal produced by large populations of short-period solar-mass binary systems of compact objects. We estimate that the primordial background can be observed only if its fractional energy density $h_{100}^2\Omega$ is greater than $\approx 5\times 10^{-13}$. The key conclusion of our analysis is that the stochastic radiation from unresolved binary systems sets a fundamental limit on the sensitivity that can be achieved in searching for the primordial background in frequencies between $\sim 10^{-6}$ Hz and 0.1 Hz, regardless of the instrumental noise level and the integration time. Indeed, the mHz frequency band, where LISA achieves optimal sensitivity, is not suitable to probe slow-roll inflationary models. We briefly discuss possible follow-up missions aimed at the frequency region ~ 0.1–1 Hz, which is likely to be free from stochastic backgrounds of astrophysical origin: no fundamental limits seem to prevent us from reaching $h_{100}^2\Omega \sim 10^{-16}$, although the technological challenges are considerable and deserve careful study.

DOI: 10.1103/PhysRevD.63.064030 PACS number(s): 04.30.−w, 04.80.Nn

I. INTRODUCTION

The Universe became ''thin'' to gravitational waves (GWs) at the Planck epoch, corresponding to the cosmic time $\sim 10^{-43}$ sec; the gravitons decoupled from the surrounding plasma at a temperature of the order of the Planck mass $\sim 10^{19}$ GeV and gravitational radiation produced at that epoch or later—including the electro-weak and the grand unified theory (GUT) scale—has traveled undisturbed to us, carrying full information about the state of the Universe and the physical processes from which it took origin. Indeed GW experiments will open radically new frontiers for cosmology and high energy physics (see [1,2] and references therein for an extensive discussion).

In the time frame $\sim$ 2002–2010 a large portion of the GW spectrum will progressively become accessible, mainly through large-scale laser interferometers. On the ground, the worldwide network of km-size interferometers—the Laser Interferometric Gravitational Wave Observatory (LIGO), GEO600, VIRGO and TAMA—sensitive in the frequency band ~ 10 Hz to 1 kHz, will start carrying out ''science runs'' at the beginning of 2002, with the realistic goal of directly detecting GWs. Several instrumental upgrades, starting around 2005, will drive the sensitivity of the instruments to a GW stochastic background from $h_{100}^2\Omega \sim 10^{-6}$ (for the so-called initial generation) to $h_{100}^2\Omega \sim 10^{-10}$ (for the so-called advanced configuration). In space, a collaboration between ESA and NASA is carrying out the project called LISA (Laser Interferometer Space Antenna). This is a space-borne laser interferometer with arms of length 5×10^6 km, planned to fly by 2010 [3]. This instrument guarantees the detection of GW at low frequencies ($\sim 10^{-5}$–10^{-2} Hz).

The purpose of this paper is to show the central role of the experiments in the low-frequency window $\sim 10^{-6}$–1 Hz, with emphasis on instruments of the LISA class, in the search for the primordial GW background. Our aim is to identify the fundamental issues regarding the achievement of a sensitivity in the range $h_{100}^2\Omega \sim 10^{-16}$–$10^{-15}$, which is set by the theoretical prediction of ''slow-roll'' inflationary models.

*Electronic address: carlo.ungarelli@port.ac.uk
†Electronic address: vecchio@aei-potsdam.mpg.de

A. Stochastic background spectrum

A stochastic GW background is a random process that can be described only in terms of its statistical properties. Without loss of generality, for the issues discussed in this paper, we assume it to be isotropic, stationary, Gaussian and unpolarized. The energy and spectral content of a stochastic background are described by the dimensionless function

$$\Omega(f) \equiv \frac{1}{\rho_c} \frac{d\rho_{gw}(f)}{d \ln f}; \tag{1.1}$$

ρ_{gw} is the energy density carried by the background radiation, and

$$\rho_c = \frac{3H_0^2 c^2}{8\pi G_N} \approx 1.6\times 10^{-8} h_{100}^2 \ \text{erg/cm}^3, \approx 1.2\times 10^{-36} h_{100}^2 \ \text{sec}^{-2} \tag{1.2}$$

is the *critical energy density* required today to close the Universe. The value of the Hubble constant (today) is

$$H_0 = 100 h_{100} \ \ \text{km sec}^{-1} \ \text{Mpc}^{-1} \simeq 3.2\times 10^{-18} h_{100} \ \text{sec}^{-1}, \tag{1.3}$$

where h_{100} is known from observations to be in the range $0.4 \leqslant h_{100} \leqslant 0.85$. Here $\Omega(f)$ is therefore the ratio of the GW energy density to the critical energy density per unit logarithmic frequency interval; one usually refers to $h_{100}^2 \Omega(f)$, which is independent of the *unknown* value of the Hubble constant.

It is useful to introduce the *characteristic amplitude* $h_c(f)$ of the GW background: it is the dimensionless characteristic value of the total GW background-induced fluctuation $h(t)$ at the output of an interferometer per unit logarithmic frequency interval:

$$\langle h^2(t) \rangle = 2 \int_0^\infty d(\ln f) h_c^2(f); \tag{1.4}$$

here $\langle\rangle$ denotes the expectation value. The spectral density $S(f)$ of the background is related to $h_c(f)$ by [1]

$$h_c^2(f) = 2 f S(f), \tag{1.5}$$

and $\Omega(f)$, $h_c(f)$, and $S(f)$ satisfy the relation [1]

$$\Omega(f) = \frac{2\pi^2}{3H_0^2} f^2 h_c^2(f) = \frac{4\pi^2}{3H_0^2} f^3 S(f). \tag{1.6}$$

The characteristic amplitude over a frequency band Δf is therefore

$$h_c(f,\Delta f) = h_c(f) \left(\frac{\Delta f}{f}\right)^{1/2} \simeq 7.1\times 10^{-22} \left[\frac{h_{100}^2 \Omega(f)}{10^{-8}}\right]^{1/2} \left(\frac{f}{1\,\text{mHz}}\right)^{-3/2} \times \left(\frac{\Delta_b f}{3.2\times 10^{-8} \ \text{Hz}}\right)^{1/2}, \tag{1.7}$$

where $\Delta_b f \simeq 3.2\times 10^{-8} (1 \ \text{yr}/T)$ Hz is the width of the frequency bin for an observation time T. For comparison, the relevant characteristic amplitude of the LISA noise is $\sim 10^{-24}$.

B. Sources of stochastic backgrounds

The stochastic GW background can be divided into two broad classes, based on its origin: (i) the *primordial GW background* (PGB), produced by physical processes in the early Universe, and (ii) the *astrophysically generated GW background* (GGB), generated by the incoherent superposition of gravitational radiation produced, at much later cosmic times, by a large number of astrophysical sources that cannot be resolved individually. The emphasis of this paper is on the detectability of the PGB.

In this paper we will use the following conventions: $\Omega_p(f)$ and $\Omega_g(f)$ identify the fractional energy density in GWs, Eq. (1.1), carried by the primordial and the generated component of the GW background, respectively. If no index is used, we refer to a general GW stochastic signal, with no assumption about its production mechanism.

At present, there are three observational constraints on the PGB contribution to $\Omega(f)$:

(1) The high degree of isotropy of the cosmic microwave background (CMB) radiation sets a limit at ultra-low frequencies [4]:

$$h_{100}^2 \Omega_p(f) < 7\times 10^{-11} \left(\frac{f}{H_0}\right)^{-2}, \qquad 3\times 10^{-18} h_{100} \ \text{Hz} \lesssim f \lesssim 10^{-16} h_{100} \ \text{Hz}. \tag{1.8}$$

(2) The very accurate timing of millisecond radio-pulsars constrains $\Omega_p(f)$ in a frequency range of the order of the inverse of the observation time, typically of order of a few years [5]:

$$h_{100}^2 \Omega_p(f) < 10^{-8}, \quad f \sim 10^{-8} \ \text{Hz}. \tag{1.9}$$

(3) The standard model of big-bang nucleosynthesis constrains the total energy content in GWs over a wide frequency range [6]:

$$\int_{f=10^{-8} \ \text{Hz}}^\infty h_{100}^2 \Omega_p(f) d(\ln f) < 6\times 10^{-6}. \tag{1.10}$$

To foresee what physical processes could have produced a detectable GW background is an almost impossible challenge; nonetheless, it is enlightening to discuss some general

principles and possible generation mechanisms to show the typical sensitivity that experiments should achieve in order to test different models.

The main mechanisms that produce a PGB can be divided into two broad categories (for a recent detailed review see [1]): (i) Parametric amplifications of metric tensor perturbations that occurred during an inflationary epoch and (ii) some causal processes—such as phase transitions—that took place in the early Universe.

Stochastic backgrounds produced by the parametric amplification of metric tensor perturbations that occurs during an inflationary epoch [7] extend over a huge range of frequencies, from $\sim 3\times 10^{-18}$ Hz up to a cutoff frequency in the GHz range. In the window $\sim 10^{-16}$ Hz to 1 GHz, slow-roll inflationary models predict a quasi-scale-invariant spectrum whose typical magnitude—in order to satisfy the bound set by CMB experiments—cannot exceed $h_{100}^2\Omega_p \sim 10^{-14}$ in the LISA frequency band, as well as in the Earth-based detectors observational window [8]; a more refined analysis [9] yields a more conservative upper limit: $h_{100}^2\Omega_p \sim 10^{-16}$–$10^{-15}$. Superstring-inspired cosmological models [10–12] predict a spectrum that, for suitable choices of the free parameters of the model, could reach $h_{100}^2\Omega_p \sim 10^{-7}$ at the frequencies accessible either to Earth-based or to space-borne experiments, while satisfying the existing observational bound [13–17].

Stochastic backgrounds can also be produced by some classical causal processes that took place in the early Universe; for this class of signals, the characteristic frequency is related both to the time of emission and the corresponding temperature $\mathcal{T}$.

Non-equilibrium processes that occur at the reheating that takes place after inflation could provide a stochastic background with cutoff frequency in the range ~ 0.1 mHz to 1 kHz, corresponding to reheating temperatures between ~ 1 TeV and $\sim 10^9$ GeV. As an example, in hybrid and extended inflationary models, the exit towards a radiation-dominated era is characterized by a first-order phase transition, which, if strongly of the first order, generates a stochastic background with $h_{100}^2\Omega_p \sim 10^{-6}$ at frequencies that can vary from the LISA observational window up to the sensitivity band of Earth-based interferometers [18].

Phase transitions that inevitably occur at $\mathcal{T}\sim 10^2$ MeV (the QCD phase transition) and $\mathcal{T}\sim 10^2$ GeV (the electroweak phase transition) produce GWs. In particular, if the electroweak phase transition is strongly of the first order, the spectrum is approximately $h_{100}^2\Omega_p \sim 10^{-11}$–$10^{-9}$ at $f \sim 1$ mHz [19]; the requirement of a strong first order phase transition, which is necessary in order to have baryogenesis at the electroweak scale (see [20] and references therein for a recent review), is directly related, in a minimal supersymmetric extension of the standard model, to the mass of the super-partner of the top quark [21–23].

Cosmic strings, which are topological defects formed during phase transitions, produce GWs whose typical frequency ranges from $f\sim 10^{-8}$ Hz up to $f\sim 10^{10}$ Hz with $h_{100}^2\Omega_p \sim 10^{-9}$–$10^{-8}$; see [24] and references therein for a review.

Global phase transitions associated with some scalar field which acquires a non-zero vacuum expectation value (VEV) below a critical temperature would produce, via a quite general relaxation process, GWs whose energy content is very significant, $h_{100}^2\Omega_p \sim 10^{-6}$, for VEVs near the Planck or string scale [25,26].

Recently there has been a great amount of theoretical activity investigating higher dimensional ''brane-world'' scenarios, where gravity begins to probe the extra dimensions at energies as low as 10^3 GeV; and an estimate of possible GW backgrounds in such models was presented recently in [27].

These examples clearly show that investigation of the primordial GW stochastic background in the low-frequency regime would provide us key information about the physics beyond the standard model and/or could allow us to discriminate between different inflationary cosmological models.

C. Detecting a stochastic background

A stochastic background is a random process which is intrinsically indistinguishable from the detector noise. In order to detect such a signal, the optimal signal processing strategy calls for correlations between two (or more pairs of) instruments, possibly widely separated in order to minimize the effects of *common* noise sources. The relevant data analysis issues have been thoroughly addressed in [28,29]; here we simply review the main concepts, and refer to [28,29], and references therein, for more details.

The statistical analysis is based on the following assumptions: the signal and the detector noise are uncorrelated; the noise in each detector is stationary and Gaussian, and possible noise correlations between two detectors are negligible.

We define the output (signal + noise) of the two instruments as $o_1(t)$ and $o_2(t)$; the cross-correlation signal C that one constructs is therefore of the form

$$C \equiv \int_{-T/2}^{T/2} dt \int_{-T/2}^{T/2} dt' o_1(t) o_2(t') Q(t-t'), \quad (1.11)$$

where $Q(t-t')$ is a suitable filter function. In the general case, the filter function depends on t *and* t' independently, that is $Q=Q(t,t')$; here we have used the property of the signal of being stationary, and therefore $Q(t,t')=Q(t-t')$. The signal-to-noise ratio (SNR) is defined as

$$\mathrm{SNR} = \frac{\mu}{\sigma}, \quad (1.12)$$

where μ and σ are the mean value and the variance of the observable C:

$$\mu \equiv \langle C \rangle = T\left(\frac{3H_0^2}{20\pi^2}\right)(\tilde{Q},\tilde{A}), \quad (1.13)$$

$$\sigma^2 \equiv \langle C^2 \rangle - \langle C \rangle^2 = \frac{T}{4}(\tilde{Q},\tilde{Q}). \quad (1.14)$$

Equations (1.13) and (1.14) are written in terms of the usual *inner product* [29]

$$(a,b)\equiv\int_{-\infty}^{+\infty}df\tilde{a}^*(f)\tilde{b}(f)R(f), \tag{1.15}$$

where $\tilde{Q}(f)$ is the Fourier transform of $Q(t-t')$. The functions $R(f)$ and $\tilde{A}(f)$ are defined as follows:

$$R(f)\equiv S_n^{(1)}(f)S_n^{(2)}(f)\left\{1+\left(\frac{3H_0^2}{10\pi^2}\right)\frac{\Omega(f)}{f^3}\left[\frac{S_n^{(1)}(f)+S_n^{(2)}(f)}{S_n^{(1)}(f)S_n^{(2)}(f)}\right]+\left(\frac{3H_0^2}{10\pi^2}\right)^2\frac{\Omega^2(f)[1+\gamma(f)^2]}{f^6S_n^{(1)}(f)S_n^{(2)}(f)}\right\}, \tag{1.16}$$

$$\tilde{A}(f)\equiv\frac{\gamma(f)\Omega(f)}{f^3R(f)}. \tag{1.17}$$

In Eq. (1.16), $S_n^{(k)}(f), k=1,2$, is the one-sided noise power spectral density of the kth detector, and $\gamma(f)$ is the so-called *overlap reduction function*, which depends entirely on the relative orientation and location of the two detectors; it accounts for SNR losses that occur when the instruments are not optimally located and oriented; cf. Eq. (1.20) and Sec. II.

Using Eqs. (1.13) and (1.14), one can cast Eq. (1.12) in the form

$$\mathrm{SNR}^2=T\left(\frac{3H_0^2}{10\pi^2}\right)^2\frac{(\tilde{Q},\tilde{A})^2}{(\tilde{Q},\tilde{Q})}. \tag{1.18}$$

The optimal choice of the filter $\tilde{Q}$ is thus based on the maximizing the SNR, Eq. (1.18), and is given by

$$\tilde{Q}(f)=(\mathrm{const})\times\tilde{A}(f), \tag{1.19}$$

where the overall normalization factor is arbitrary. Note that Eqs. (1.11)–(1.19) are valid for a background of arbitrary energy density $\Omega(f)$. In the case of a signal much weaker than the noise, $H_0^2\Omega(f)/f^3\ll S_n^{(k)}(f)$, one can Taylor expand Eqs. (1.16) and (1.17), retaining only the leading order term. As a consequence, Eq. (1.18) reduces to

$$\mathrm{SNR}\simeq\frac{3H_0^2}{\sqrt{50}\pi^2}T^{1/2}\times\left[\int_0^\infty df\frac{\gamma(f)^2\Omega^2(f)}{f^6S_n^{(1)}(f)S_n^{(2)}(f)}\right]^{1/2}\quad(\mathrm{signal}\ll\mathrm{noise}). \tag{1.20}$$

It is convenient to introduce the noise characteristic amplitude h_{rms}, equivalent to h_c, as follows:

$$\langle n^2(t)\rangle=\int_0^\infty dfS_n(f)=2\int_0^\infty d(\ln f)h_{\mathrm{rms}}^2(f). \tag{1.21}$$

It is enlightening to write Eq. (1.20), using Eqs. (1.4) and (1.21), in the form

$$\mathrm{SNR}\sim\gamma(f_c)(\Delta fT)^{1/2}\left[\frac{h_c(f_c)}{h_{\mathrm{rms}}(f_c)}\right]^2; \tag{1.22}$$

here we have assumed that the frequency band Δf, which contains most of the SNR, is centered on the characteristic frequency f_c, and is sufficiently small; the noise spectral density of the two instruments, which for simplicity we assume identical, and the overlap reduction function can be therefore treated as roughly constant. If only one instrument is in operation, one could in principle detect a stochastic background with $\mathrm{SNR}\gtrsim 1$ when $h_c\gtrsim h_{\mathrm{rms}}$; with two instruments one can detect the signal when $h_c\gtrsim h_{\mathrm{rms}}/[\gamma(f_c)\times(\Delta fT)^{1/4}]$. Cross-correlation experiments are therefore highly desirable for both detection confidence and sensitivity. In fact, one can isolate the stochastic GW signal from all the spurious contributions which are uncorrelated between the two instruments. Common noise sources, which correlate on the same light-travel time scale, might, however, be present, degrading the overall sensitivity. Moreover, GW signals are expected to be very weak, well buried into the noise; using cross-correlations, through optimal filtering, one increases the sensitivity by a factor $\sim 10\ (\Delta f/1\ \mathrm{mHz})^{1/4}\ (T/10^7\ \mathrm{sec})^{1/4}$, with respect to the single detector case.

D. Summary of the results

The goal of this paper is to explore the capability of space-borne laser interferometers, such as LISA and its successors, in searching for the primordial GW stochastic backgrounds. The analysis of the LISA technology leads us to the following conclusions:

(i) A PGB of fractional energy density $h_{100}^2\Omega_p\gtrsim 10^{-10}$ definitely shows up as an excess power component in the data of a single LISA interferometer over a large frequency window; it might be detectable by calibrating the noise-only response of the instrument, but the issue of decisively assigning this contribution to a real primordial signal remains open.

(ii) Cross-correlations between the data streams of two identical LISAs, characterized by the presently estimated instrumental noise, allow us to reach a minimum value of the fractional energy density carried by GWs in the range $5\times 10^{-14}\lesssim h_{100}^2\Omega^{(\mathrm{min})}\lesssim 10^{-12}$ for an integration time $T=10^7$ sec, depending on the location and orientation of the two detectors.

(iii) Such remarkable sensitivity, however, does not apply to *primordial* GW backgrounds; in fact, the copious number of short period solar-mass binary systems in the Universe produce a GGB that overwhelms the PGB in the key mHz region; we estimate that *the minimum detectable value of the primordial GW background is* $h_{100}^2\Omega_p^{(\mathrm{min})}\gtrsim 5\times 10^{-13}$.

(iv) The cross-correlation of the data streams from two LISA detectors provides, therefore, a powerful tool to extract information about populations of binary systems of short-period solar-mass compact objects in the Universe: the GGB is detectable at a signal-to-noise ratio ~ 100.

We would like to emphasize that the third generation Earth-based laser interferometers, instruments such as advanced LIGO (LIGO III) and EUGO, a new European detector currently under study, will be able to achieve a sensitivity

$h_{100}^2\Omega^{(\min)} \sim 10^{-10}$; space-based interferometers will therefore play a primary role in GW cosmology.

Although the former results are very encouraging, our analysis leads to the rather obvious, but somewhat disappointing, outcome that experiments in the frequency band $\sim 10^{-6}$ Hz–0.1 Hz will be limited to a sensitivity of the order $h_{100}^2\Omega_p \sim 10^{-13}$–$10^{-12}$; this limit cannot be improved by reducing the instrumental noise and/or increasing the integration time; in fact, GGB's produce a residual correlation in the filter output designed to detect the PGB that cannot be eliminated: *the mHz frequency window is not suitable to search for a primordial gravitational wave background characterized by* $h_{100}^2\Omega_p < 5\times 10^{-13}$.

It is therefore worth asking whether future technological developments and more ambitious missions will enable the detection of a very weak PGB. Our present understanding suggests that cross-correlation experiments carried out with a pair of space-based interferometers with optimal sensitivity in the band ~ 0.1–1 Hz could be able to meet the target $h_{100}^2\Omega_p \sim 10^{-16}$. In this frequency band, in fact, astrophysically generated backgrounds are not present, and an experiment is limited in principle only by the instrumental noise. The design of a detector aimed at the window ~ 0.1–1 Hz imposes stringent requirements on the power and frequency of the laser, as well as on the dimensions of the ''optics'' and on several other components of the instrument. In order to test slow-roll inflation an effective—i.e., after residual radiation from individual binary systems has been removed—rms noise level $\sim 10^{-24}$ and rather long integration times (≈ 3 years) are required. Such technological and data analysis issues have been little investigated so far, and deserve careful consideration.

The paper is organized as follows. In Sec. II we derive a closed form expression of the overlap reduction function for a pair of space-based interferometers. In Sec. III we review our present astrophysical understanding of the GW background generated by the incoherent superposition of radiation emitted by galactic and extra-galactic short period solar-mass binary systems. In Sec. IV we present the key results of the paper: we estimate the sensitivity that can be achieved by the present LISA technology, and possible follow-up missions, by cross-correlating the outputs of two identical detectors with uncorrelated noise. Section V contains our conclusions and some pointers to future work.

II. OVERLAP REDUCTION FUNCTION FOR LISA DETECTORS

In this section we compute a closed form expression for the overlap reduction function $\gamma(f)$ [see Eqs. (1.16)–(1.19)], for space-borne interferometers and in particular for instruments characterized by a LISA-like orbital configuration. Indeed, our analysis provides explicit formulas that can be directly applied, with little changes, to any orbital configuration.

The overlap reduction function is a dimensionless function of the frequency f, which measures the degradation of the SNR when the detectors are not optimally oriented and located. At any given frequency, $\gamma(f)$ depends entirely on the relative separation and orientation of the instruments, and its behavior has a very intuitive physical explanation. It is maximum when the detectors are co-located and co-aligned. As the detectors (parallel to each other) are shifted apart, at a distance D, the signal drives oscillations in the two instruments that are progressively out of phase; there is an effective correlation only if the separation is smaller than approximately half of the characteristic wavelength of the gravitational radiation; equivalently, the frequency band over which one accumulates SNR is

$$f \lesssim 1 \left(\frac{D}{1\ \mathrm{AU}} \right)^{-1} \ \mathrm{mHz}, \tag{2.1}$$

where one astronomical unit (AU) corresponds to 1.4959787×10^{13} cm. For two coincident detectors, $\gamma(f)$ decreases, at any frequency, as one instrument is rotated with respect to the other, because the detectors are excited in different ways by the different polarizations; for a rotation of $\pi/4$, the overlap reduction function is identically zero. In the general case, $\gamma(f)$ shows a complex behavior which is the superposition of the two effects that we have just described.

A. LISA mission

LISA is an all-sky monitor with a quadrupolar antenna pattern. Its orbital configuration was conceived in order to keep the geometry of the interferometer as stable as possible during the mission, as well as to provide an optimal coverage of the sky: a constellation of three drag-free spacecraft (containing the free-falling test masses) is placed at the vertices of an ideal equilateral triangle with sides $\simeq 5\times 10^6$ km; it forms a three-arm interferometer, with a 60° angle between two adjacent laser beams. The LISA orbital motion is such that the barycenter of the instrument is inserted in a heliocentric (essentially circular) orbit, following by 20° the Earth; the detector plane is tilted by 60° with respect to the Ecliptic and the instrument counter-rotates around the normal to the detector plane with the same period of 1 yr.

We introduce a Cartesian reference frame (x,y,z) tied to the Ecliptic, with $\hat{\mathbf{z}}$ perpendicular to the Ecliptic plane, and $\hat{\mathbf{x}}$ and $\hat{\mathbf{y}}$ in the plane itself, and oriented in such a way to define a left-hand term. In this frame, LISA's center of mass is described by the polar angles

$$\Theta = \frac{\pi}{2}, \quad \Phi(t) = \Phi_0 + n_\oplus t, \quad \left(n_\oplus \equiv \frac{2\pi}{1\ \mathrm{yr}} \right); \tag{2.2}$$

Φ_0 sets the position of the detector barycenter at some arbitrary reference time. The time evolution of the unit vectors $\hat{\mathbf{l}}_j$ $(j=1,2,3)$ along each arm is described by the following expression [30]:

$$\begin{aligned} \hat{\mathbf{l}}_j = & \left[\frac{1}{2}\sin\alpha_j(t)\cos\Phi(t) - \cos\alpha_j(t)\sin\Phi(t) \right] \hat{\mathbf{x}} \\ & + \left[\frac{1}{2}\sin\alpha_j(t)\sin\Phi(t) + \cos\alpha_j(t)\cos\Phi(t) \right] \hat{\mathbf{y}} \\ & + \left[\frac{\sqrt{3}}{2}\sin\alpha_j(t) \right] \hat{\mathbf{z}}, \end{aligned} \tag{2.3}$$

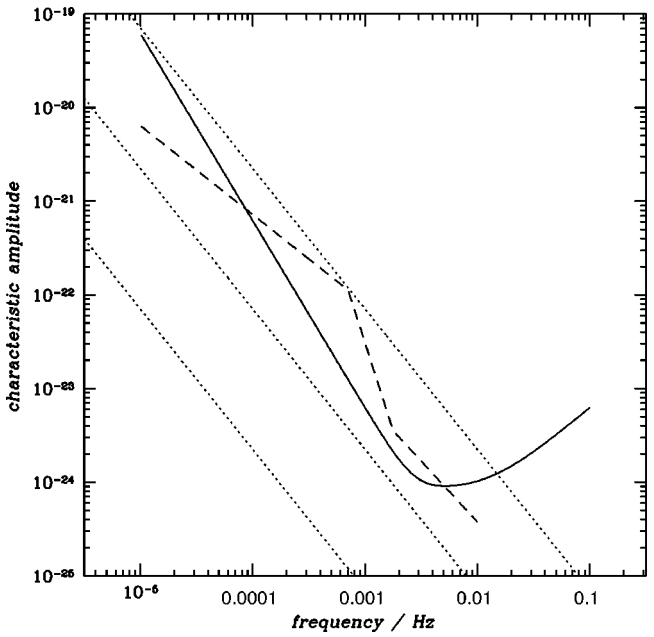

FIG. 1. The characteristic amplitude of stochastic gravitational wave backgrounds of primordial and astrophysical origin and the LISA rms noise amplitude. The plot shows the LISA rms noise amplitude in one year of observation (solid line), as a function of frequency, and compares it to the characteristic amplitude of several stochastic signals: a background with flat spectrum $h_{100}^2\Omega=10^{-10}$, 10^{-13}, 10^{-16} (dotted lines, from top to bottom, respectively) and the astrophysically generated galactic background (dashed line), according to the estimate given by Bender and collaborators; cf. Eq. (3.1).

where $\alpha_j(t)$ increases linearly with time according to

$$\alpha_j(t)=n_{\oplus}t-(j-1)\pi/3+\alpha_0, \tag{2.4}$$

and α_0 is just a constant specifying the orientation of the arms at the arbitrary reference time $t=0$.

In the next section we will derive the expression of the overlap reduction function for two detectors characterized by a LISA-like motion. The time dependence of $\hat{\mathbf{l}}_j$ and the center of mass are described by Eqs. (2.2), (2.3) and (2.4) for both instruments, just with different initial conditions α_0 and Φ_0. We will use the notation α_{01}, Φ_{01}, and α_{02}, Φ_{02} to indicate the corresponding values of detectors ''1'' and ''2,'' respectively. For future convenience, we also introduce the notation

$$\Delta\Phi_0=\Phi_{02}-\Phi_{01}, \quad \Delta\alpha_0=\alpha_{02}-\alpha_{01}. \tag{2.5}$$

The main noise sources that affect the mission have been addressed by the LISA Science Team and yield the following expression for the expected noise spectral density [3]:

$$S_n(f)\simeq 10^{-48}[1.22\times10^{-3}f^{-4}+16.74+9.7\times10^4 f^2]\ \ \mathrm{Hz}^{-1}; \tag{2.6}$$

the rms noise amplitude that is inferred from $S_n(f)$ is shown in Fig. 1.

B. Overlap reduction function

To derive a closed form expression of the overlap reduction function $\gamma(f)$, we follow the formalism developed by Allen and Romano [29], which in turn was based on the analysis done by Flanagan [28]. $\gamma(f)$ is formally given by

$$\gamma(f)=\rho_1(x)d_{ab}^{(1)}d^{(2)ab}+\rho_2(x)d_{ab}^{(1)}S^b d^{(2)ac}S_c + \rho_3(x)d_{ab}^{(1)}d_{cd}^{(2)}S^a S^b S^c S^d. \tag{2.7}$$

In the previous expression, $d_{ab}^{(k)}$ are the *detector response tensors*, defined as

$$d_{ab}^{(k)}=\frac{1}{2}[m_a^{(k)}m_b^{(k)}-n_a^{(k)}n_b^{(k)}], \tag{2.8}$$

where $k=1,2$ labels the instrument, and $\hat{\mathbf{m}}^{(k)}$ and $\hat{\mathbf{n}}^{(k)}$ are the unit vectors along the arms of the interferometers; our (arbitrary) choice corresponds to $\hat{\mathbf{l}}_1$ and $\hat{\mathbf{l}}_2$, respectively, given by Eqs. (2.3) and (2.4), with the appropriate initial conditions. The unit vector along the direction that connects the centers of mass of the two detectors is

$$\hat{\mathbf{S}}=\frac{\cos\Phi_2-\cos\Phi_1}{\sqrt{2[1-\cos(\Phi_2-\Phi_1)]}}\,\hat{\mathbf{x}}+\frac{\sin\Phi_2-\sin\Phi_1}{\sqrt{2[1-\cos(\Phi_2-\Phi_1)]}}\,\hat{\mathbf{y}}; \tag{2.9}$$

x is a dimensionless parameter defined as

$$x\equiv\frac{2\pi fD}{c}, \tag{2.10}$$

where

$$D=R_{\oplus}\sqrt{2(1-\cos\Delta\Phi_0)}, \tag{2.11}$$

and the functions $\rho_j(x)$ are given by

$$\rho_1(x)=5j_0(x)-\frac{10}{x}j_1(x)+\frac{5}{x^2}j_2(x),$$

$$\rho_2(x)=-10j_0(x)+\frac{40}{x}j_1(x)-\frac{50}{x^2}j_2(x),$$

$$\rho_3(x)=\frac{5}{2}j_0(x)-\frac{25}{x}j_1(x)+\frac{175}{2x^2}j_2(x), \tag{2.12}$$

where

$$j_0(x)=\frac{\sin x}{x},$$

$$j_1(x)=\frac{\sin x}{x^2}-\frac{\cos x}{x},$$

$$j_2(x)=3\frac{\sin x}{x^3}-3\frac{\cos x}{x^2}-\frac{\sin x}{x} \tag{2.13}$$

are the standard spherical Bessel functions.

By substituting Eq. (2.3) into Eq. (2.8), and combining it with Eqs. (2.9)–(2.13), one can derive the following expressions:

$$d^{(1)}_{ab}d^{(2)ab}=\sum_{k=0}^{4}\,[A_k\cos(2\Delta\alpha_0+k\Delta\Phi_0) + B_k\sin(2\Delta\alpha_0+k\Delta\Phi_0)],, \tag{2.14}$$

$$d^{(1)}_{ab}S^b d^{(2)ac}S_c=\sum_{k=0}^{4}\,[C_k\cos(2\Delta\alpha_0+k\Delta\Phi_0) + D_k\sin(2\Delta\alpha_0+k\Delta\Phi_0)], \tag{2.15}$$

$$d^{(1)}_{ab}d^{(2)}_{cd}S^aS^bS^cS^d=\sum_{k=0}^{4}\,[E_k\cos(2\Delta\alpha_0+k\Delta\Phi_0) + F_k\sin(2\Delta\alpha_0+k\Delta\Phi_0)], \tag{2.16}$$

where $\Delta\alpha_0$ and $\Delta\Phi_0$ are given by Eq. (2.5), and A_k, B_k, C_k, D_k, E_k and F_k (for $k=0,\ldots,4$) are numerical coefficients, which are given in the Appendix. Inserting Eqs. (2.14),(2.16) into Eq. (2.7), the overlap reduction function becomes

$$\gamma(f)=\sum_{k=0}^{4}\,[P_k(x)\cos\varphi_k(\Delta\alpha_0,\Delta\Phi) + Q_k(x)\,\sin\varphi_k(\Delta\alpha_0,\Delta\Phi)] \tag{2.17}$$

where

$$P_k(x)=\rho_1(x)A_k+\rho_2(x)C_k+\rho_3(x)E_k,$$

$$Q_k(x)=\rho_1(x)B_k+\rho_2(x)D_k+\rho_3(x)F_k \tag{2.18}$$

depend only on the detector separation and the radiation frequency, and

$$\varphi_k(\Delta\alpha_0,\Delta\Phi_0)\equiv 2\Delta\alpha_0+k\Delta\Phi_0 \tag{2.19}$$

is a function of the relative orientation of the instruments.

We would like to stress that our definition is such that $\gamma(f)=1\ \forall f$, *for co-aligned and co-located interferometers with arms perpendicular to each other*; that is, the angle between $\hat{\mathbf{m}}$ and $\hat{\mathbf{n}}$ is $\pi/2$. However, the LISA opening angle is $\pi/3$, and the detector response is reduced by the factor $\sqrt{3}/2$: as a consequence, the maximum value that $\gamma(f)$ can attain is 3/4.

Notice also that, as pointed out by Cutler [30], the readouts from the three arms of LISA can be combined in such a way to form the outputs, say o_I and o_{II}, of two co-located interferometers rotated by $\pi/4$, one with respect to the other, whose noise is uncorrelated at all frequencies. Unfortunately, the cross-correlation of o_I with o_{II} is useless for searching for stochastic backgrounds, as the overlap reduction function is identically zero over the whole frequency range.

Figures 2 and 3 show the behavior of $\gamma(f)$ as a function of the frequency and the separation angle $\Delta\Phi_0$, which is

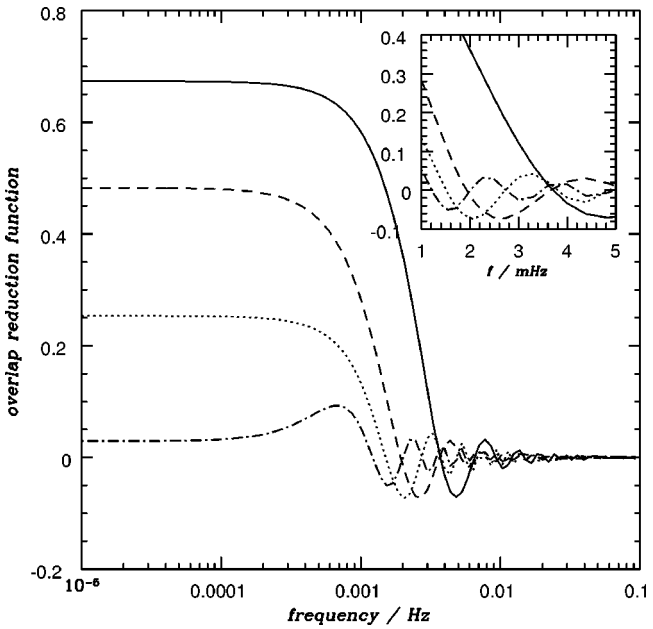

FIG. 2. The overlap reduction function $\gamma(f)$ for a pair of identical laser interferometers with the LISA orbital configuration. The plot shows $\gamma(f)$ as a function of the frequency for four different center-of-mass separation angles $\Delta\Phi_0$, which correspond to different distances of the two detectors [cf. Eq. (2.11)]: $\Delta\Phi_0=20°$ (solid line), $\Delta\Phi_0=40°$ (dashed line), $\Delta\Phi_0=60°$ (dotted line), $\Delta\Phi_0=90°$ (dot-dashed line). Here we always assume that the initial orientation of the detectors is such that $\Delta\alpha_0=0$. The small panel at the top zooms the behavior of $\gamma(f)$ in the mHz region.

equivalent to the distance D; see Eq. (2.11). Here we assume that the instruments are inserted into their orbits so that $\Delta\alpha_0=0$. In this case, at fixed frequency, the overlap reduction function depends only on $\Delta\Phi_0$, as the relative orientation of the detectors is determined only by $\Phi(t)$; cf. Eqs. (2.3) and (2.4). This also implies that as the two instruments are moved apart—$\Delta\Phi_0$ increases—their orientation changes too. In order to achieve the maximum $\gamma(f)$ for a given separation, one should therefore suitably tune the initial orientation of the detector arms. The plots clearly show that at low frequencies, $f\lesssim 5\times10^{-4}$ Hz, $\gamma(f)$ is fairly flat and close to its maximum value (which is set by the separation and orientation); in fact the radiation wavelength is $\lambda_{gw}\simeq 2(f/1\ \mathrm{mHz})^{-1}$ AU, and for separations smaller than 1 AU, the degradation of SNR at very low frequencies is less than a factor of ≈ 2. At high frequencies, say $f\gtrsim 10^{-2}$ Hz, placing two interferometers at a distance larger than 10^6 km would severely degrade the SNR by a factor of 10 or more.

III. ASTROPHYSICALLY GENERATED STOCHASTIC BACKGROUND

The so-called *astrophysically generated GW stochastic background* (GGB) is mainly due to the incoherent superposition of gravitational radiation emitted by short-period solar-mass binary systems. A variety of binary populations contribute to it, but the main contribution, in the mHz region, is due to close white-dwarf binaries (CWDBs). Present esti-

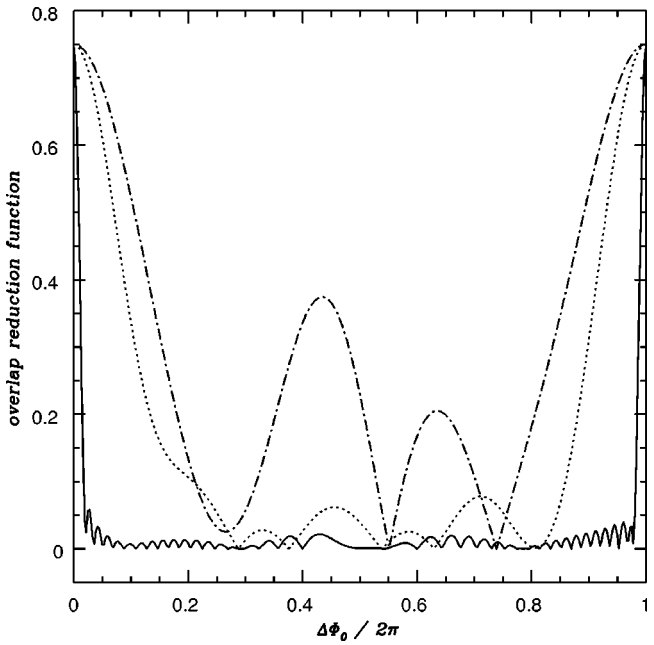

FIG. 3. The overlap reduction function for a pair of identical laser interferometers with the LISA orbital configuration. The plot shows $\gamma(f)$ as a function of center-of-mass separation angle $\Delta\Phi_0$ (in units 2π), for selected frequencies: $f=10^{-2}$ Hz (solid line), $f=10^{-3}$ Hz (dotted line), and $f=10^{-4}$ Hz (dot-dashed line). The constants α_{01} and α_{02} are selected in such a way that, at the (arbitrary) reference time $t=0$, $\Delta\alpha_0=0$.

mates suggest that it is above the LISA instrumental noise in the frequency region $\approx 10^{-4}$–3×10^{-3} Hz, right at the heart of the observation window; see Fig. 1. However, sizable effects are also given by other sources such as W UMa (Ursae Majoris) binary stars, unevolved binaries, cataclysmic binaries, neutron-star–neutron-star (NS-NS) binary systems, black-hole–neutron-star (BH-NS) binaries, and possibly BH-BH binary systems.

The GGB is a *guaranteed* GW source in the low-frequency band; however, it is likely to overwhelm the PGB, degrading the sensitivity of the instruments in searching for a stochastic signal produced in the early Universe. A rigorous analysis of GGBs goes far beyond the purpose of this paper; here we review the main features and discuss the fundamental theoretical issues. We refer the reader to [31–35], and references therein, for a thorough discussion of the astrophysical sources.

Ultimately, the reason that the radiation generated by large populations of binary systems is effectively a stochastic signal is simple: there are too many free parameters that one needs to fit the data in order to *resolve* all the binary systems that contribute to the signal. In fact, our galaxy contains $\sim 10^7$ CWDBs; they evolve, due to radiation reaction, over a time scale $\gtrsim 10^7$ yr. Therefore, during the typical observation time $T\sim 1$ yr, they are seen as highly monochromatic, and, in the band 10^{-4}–10^{-3} Hz, each frequency bin is ''contaminated'' by roughly 10^3 sources. The problem of resolving each individual binary system is actually made worse by the motion of the detector, because in addition to the frequency, one needs to solve also for the source position in the sky and the orientation of the orbital plane.

In the following we discuss the estimates $\Omega_g(f)$ of the spectral energy density of generated backgrounds and, in particular, their *isotropic* component and the critical frequency f_g up to which GGBs are indeed present. For $f \gtrsim f_g$, the individual binary sources of astrophysical populations can be resolved and their radiation subtracted from the data, opening up the band to search for a PGB. The former two properties are essential in addressing the possibility of detecting PGBs with space-based experiments.

In this context, it is useful to divide the sources that contribute to the GGB into two categories: galactic sources and extra-galactic sources. Their key distinguishing feature of relevance here is the degree of isotropy of the GGB that they generate for an observer on board a LISA-like detector. In fact, the extra-galactic contribution is expected to be isotropic to a rather high degree (the radiation being dominated by binary systems at cosmological distances; for more details see [36]); it is, therefore, impossible to discriminate it from the PGB. On the contrary, the GGB produced by galactic sources is clearly highly anisotropic. In fact, galactic stars are spatially distributed, approximately, according to $\exp(-r/r_0)\exp[-(z/z_0)^2]$, where r is the radial distance to the Galactic center, $r_0\simeq 5$ kpc, and z the height above the Galactic plane; $z_0\sim 5$ kpc for neutron star binaries and less than 300 pc for the other types. As a result of the peripheral location of the Solar System, and the change of orientation of the LISA arms during the years-long observation time, galactic generated backgrounds appear strongly anisotropic [37]. It is also conceivable that the isotropic portion of the galactic contribution does not exceed the total extra-galactic GGB.

Several astrophysical uncertainties affect the estimates of the GGB that have been carried out so far. A careful analysis of the galactic contribution has been performed by Bender and collaborators [31,32], taking into account a wide range of binary populations. A good fit of the galactic GGB spectral density is

$$S_g(f)=\begin{cases} 10^{-42.685}f^{-1.9} & 10^{-5}\leqslant f\leqslant 10^{-3.15}, \\ 10^{-60.325}f^{-7.5} & 10^{-3.15}\leqslant f\leqslant 10^{-2.75}, \\ 10^{-46.85}f^{-2.6} & 10^{-2.75}\leqslant f, \end{cases} \tag{3.1}$$

which is related to $\Omega_g(f)$ by Eq. (1.6). In Eq. (3.1) the space density of CWDBs is assumed to be 10% of the theoretical value predicted by Webbink [38], and the radiation from helium cataclysmic variables, likely to contribute significantly in the frequency window $\simeq 1$ mHz–3 mHz, is not taken into account. The estimate (3.1) can be definitely regarded as a solid lower limit, and is likely correct within to a factor ~ 3; see also [33,34]. We would also like to stress that the dominant contribution from CWDBs switches off at $\sim 10^{-2}$ Hz, where the binary systems coalesce; for $f \gtrsim 10^{-2}$ Hz, NS-NS binary systems are the sources that contribute most to the GGB.

The extragalactic contribution to the GGB has been estimated in [34], and is weaker than the galactic contribution by

a factor of ≈ 10–3 in the relevant frequency band, where the main uncertainty comes from the star formation rate at high redshifts [39,40] (see however the optimistic estimates in [35]). As we have mentioned at the beginning of the section, it is likely that the total (galactic + extra-galactic) isotropic component of the GGB does not exceed the total extra-galactic GGB; indeed, we will assume that the isotropic portion of $\Omega_g(f)$, the only one that affects searches for the PGB, follows the frequency distribution predicted by Eq. (3.1), but reduced by a factor $\epsilon \leqslant 1$. In the rest of the paper we will therefore assume

$$\Omega_{g,is} = \epsilon \frac{4\pi^2}{3H_0^2} f^3 S(f). \tag{3.2}$$

Note that the determination of the value of ϵ is a delicate matter. At frequencies above a few mHz, where the GWs from galactic sources can be subtracted, it is likely that $\epsilon \lesssim 0.3$, while below ~ 1 mHz, Ref. [37] suggests $\epsilon \approx 0.7$. However, a more detailed analysis is needed in the future to provide a better estimate of this value. In the following we optimistically set $\epsilon = 0.1$, which can be regarded as a solid lower limit; the results that we will present in the next section can be easily rescaled as a function of ϵ.

We consider now the critical frequency f_g up to which radiation emitted by solar-mass binary systems (in the whole Universe) produces a GGB. For $f \gtrsim f_g$ the observational window becomes ''transparent'' to the primordial GW background. Following the discussion at the beginning of the section, we estimate f_g by using a very simple argument based on first principles: if the number of independent degrees of freedom of the data set—the number of data points or, equivalently, the number of frequency bins—is smaller than the total number of independent parameters that describe the radiation, then the superposition of monochromatic GWs must be considered as a stochastic background. If the opposite is true, we have enough information to characterize, at least in principle, each individual source, and the signal is a deterministic one. For the sake of simplicity—although not exactly true, see the discussion at the beginning of the section and [30]—we assume that each binary system is characterized by one parameter. The critical frequency f_g is, therefore, formally determined by the condition that the (average) number of sources per frequency bin be less than 1:

$$\frac{dN(f)}{df} \Delta_b f \lesssim 1; \tag{3.3}$$

here dN/df is the number of binary sources, emitting at frequency f, per unit frequency interval. Assuming that the merger rate is R and in the relevant frequency range the binaries evolve only through radiation reaction, we have

$$\frac{dN(f)}{df} \Delta_b f = \frac{R}{T} \left(\frac{df}{dt} \right)^{-1}, \tag{3.4}$$

where df/dt can be estimated using the Newtonian quadrupole formula

$$\frac{df}{dt} = \frac{96}{5} \pi^{8/3} \mathcal{M}^{5/3} f^{11/3}, \tag{3.5}$$

and $\mathcal{M} \equiv (m_1 m_2)^{3/5}/(m_1+m_2)^{1/5}$ is the so-called *chirp mass* (m_1 and m_2 are the masses of the two orbiting stars). Substituting Eqs. (3.4), and (3.5) into Eq. (3.3), the frequency f_g is easily determined:

$$f_g \simeq \left(\frac{5}{96} \right)^{3/11} \pi^{-8/11} \mathcal{M}^{-5/11} \left(\frac{R}{T} \right)^{3/11}. \tag{3.6}$$

We are now interested in determining an upper limit to f_g, considering binary populations from the whole Universe. For $f \gtrsim 10$ mHz, the main contribution to the GGB is given by NS-NS binaries [31]. Their merger rate is uncertain; current estimates yield a galactic merger rate in the range [41–43]

$$R_{\rm NS} \simeq 10^{-6} - 5 \times 10^{-4} \ \ {\rm yr}^{-1}. \tag{3.7}$$

We can extrapolate this result to the entire Universe by simply multiplying the galactic rate by the total number of galaxies N_G:

$$R \sim 10^6 \left(\frac{R_{\rm NS}}{10^{-5} \ \ {\rm yr}^{-1}} \right) \left(\frac{N_G}{10^{11}} \right) \ \ {\rm yr}^{-1}. \tag{3.8}$$

By using this approach, we assume that $R_{\rm NS}$ does not vary with the redshift, which is probably not true. However, even if at high redshift $R_{\rm NS}$ is a factor of 10 higher than in our galaxy, the very weak dependence of $f_g \propto R^{3/11}$ on the merger rate [see Eq. (3.6)] ensures that this crude estimate is correct within a factor of $\simeq 2$. Assuming that the typical chirp mass of the binaries in the population is $\bar{\mathcal{M}} = 1.2 \ M_\odot$, which corresponds to $m_1 = m_2 = 1.4 \ M_\odot$, and the rate (3.8), Eq. (3.6) yields

$$f_g \simeq 1.6 \times 10^{-1} \left(\frac{R}{10^6 \ \ {\rm yr}^{-1}} \right)^{3/11} \times \left(\frac{T}{1 \ \ {\rm yr}} \right)^{-3/11} \left(\frac{\bar{\mathcal{M}}}{1.2 \ \ M_\odot} \right)^{-5/11} \ \ {\rm Hz}. \tag{3.9}$$

This simple analysis leads therefore to the conclusion that the window $f \gtrsim 0.1$ Hz is likely free from stochastic backgrounds generated by astrophysical sources; radiation from NS-NS binaries is still present, but one can detect each individual source, estimate its parameters, and remove from the data stream the signals. In principle, the search for the PGB becomes limited only by the instrumental noise.

IV. SENSITIVITY

We can now proceed to discuss the sensitivity of LISA and possible follow-up missions to search for the PGB. The major disadvantage of the presently designed LISA mission is the lack of two instruments with uncorrelated noise; in fact, each pair of the three co-located LISA interferometers shares one arm and, therefore, common noise. One can, in

principle, extract two data streams with uncorrelated noise at all frequencies [30]. Unfortunately they are equivalent to the outputs of a pair of detectors, one rotated by 45° with respect to the other, and as we have stressed in Sec. II, the response to a stochastic signal is then null. Nonetheless, LISA can play an important role in searching for stochastic backgrounds, as it can possibly achieve a sensitivity $h_{100}^2\Omega \sim 10^{-11}$–$10^{-10}$ by exploiting some intrinsic properties of the signal and/or the unique features of the instrument to operate in a configuration where the GW signal is (almost) absent.

During the observation time, LISA changes orientation with period 1 yr. A background which is anisotropic produces a periodic modulation in the auto-correlation function that can stand above the noise [37]. Unfortunately, one cannot exploit this feature to detect a primordial signal that we expect to be intrinsically isotropic to a high degree; the only sizable anisotropy that one can foresee is a *dipolar* one, produced by the motion of our local system (and therefore LISA) with respect to the cosmological rest frame with velocity $v_{\rm prop}/c \simeq 10^{-3}$. Unfortunately, an interferometer has a quadrupolar antenna pattern, and the SNR produced by the quadrupole component is reduced by a factor $(v_{\rm prop}/c)^2 \sim 10^{-6}$. Nonetheless, the use of the signature induced by anisotropies could lead to the detection of galactic generated backgrounds, as suggested in [37].

Time delay interferometry with multiple readouts [44] provides a way of suppressing by several orders of magnitude the GW contribution from the LISA output at frequencies below a few mHz, providing a shield to GW radiation. By exploiting this feature, one can calibrate the noise-only response of the instrument, and search for an excess power in the data stream that can be assigned to a signal of cosmic origin.

LISA can therefore carry out searches for stochastic backgrounds with a single instrument at a very interesting sensitivity level. LISA is likely to detect the galactic astrophysically generated background, and could set important upper limits on the primordial contribution, which can rule out existing models. It also provides invaluable information regarding the astrophysically generated backgrounds that might turn out to be crucial in designing future follow-up missions devoted to GW cosmology.

However, in order to reach the sensitivity $h_{100}^2\Omega \sim 10^{-16}$ that we have set as a goal, two separated interferometers are essential. It is important to understand whether this target sensitivity is within the reach of near future space technology and to discuss possible fundamental limitations that might prevent us from achieving a detection at the level $h_{100}^2\Omega \sim 10^{-16}$. The science goals are of such importance that some suggestions have been already put forward as to how to introduce modifications to the currently envisaged LISA configuration in order to accommodate a pair of independent instruments, possibly with the capability of shifting at will the center of the sensitivity window from $\sim 10^{-3}$ Hz to ~ 0.1 Hz [45].

We start by considering a pair of identical LISA detectors; we therefore assume present, or near future, technology. Then, we discuss ''second generation'' LISA detectors, specifically aimed at PGB searches.

A. Sensitivity of two LISA interferometers

We consider what the present LISA technology allow us to achieve by cross-correlating the outputs of two identical interferometers located at a distance D [cf. Eq. (2.11)]; this is equivalent to determining the minimum value of $h_{100}^2\Omega$ that one is able to detect. No unique answer can be given to this question, as it depends, of course, on the frequency dependence of the true signal $\Omega(f)$. Lacking any solid theoretical prediction, we choose a ''maximum ignorance'' approach, and assume that $\Omega(f)$ is constant over the relevant frequency range. This hypothesis is not unreasonable, because the frequency band over which the SNR builds up is fairly small, due to $S(f)$ and $\gamma(f)$ [cf. Eqs. (2.6), (2.17), and Figs. 1 and 2]. By setting $\Omega(f)=\text{const}$, and $S_n^{(1)}(f)=S_n^{(2)}(f)=S_n(f)$, and solving Eq. (1.20) for Ω, we can estimate the minimum detectable value of the energy density content of the GW background:[1]

$$h_{100}^2\Omega^{(\rm min)} = \frac{K}{T^{1/2}}\frac{\sqrt{50}\pi^2}{3H_0^2}\left[\int_0^\infty \frac{\gamma^2(f)}{f^6 S_n^2(f)}\right]^{-1/2}; \qquad (4.1)$$

the constant K is related to the false alarm probability and the detection rate associated with the measurement of a background with energy $\Omega^{(\rm min)}$. For a false alarm probability of 5% and a detection rate of 95%, we have $K \simeq 3.76$ (the sum of the false alarm probability and the detection rate need not be 1, and these two quantities are totally subjective) [29]. We therefore compute Eq. (4.1), with noise spectral density and overlap reduction function given by Eqs. (2.6) and (2.17), respectively. The results presented here are computed, for sake of simplicity, for the case $\Delta\alpha_0=0$, and the integration is carried out over the frequency band 10^{-4}–10^{-2} Hz.

It is interesting to analyze first how different frequency regions of the whole sensitivity window contribute to the total SNR. Figure 4 shows the fraction of the total signal-to-noise ratio that is accumulated per unit logarithmic frequency interval; it indicates clearly that the key frequency band is $\approx 8\times10^{-4}$–5×10^{-3} Hz.

Figure 5 shows the sensitivity to a generic GW stochastic background that one could *in principle* achieve for a time of observation $T=10^7$ sec. It is straightforward to rescale these results for a different observation time, as SNR $\propto T^{1/2}$ and $h_{100}^2\Omega^{(\rm min)} \propto T^{-1/2}$; see Eqs. (1.12) and (4.1). It is remarkable that LISA is capable of measurements in the range $5\times10^{-14} \lesssim h_{100}^2\Omega^{(\rm min)} \lesssim 10^{-12}$, which is about three orders of magnitude better than can be achieved (although in a different frequency regime) with Earth-based interferometers operating in the ''advanced'' configuration. The latter experimental setup requires considerable technological and possibly conceptual developments, and is expected to be implemented not before the end of the decade. The one-

[1]Notice that it is appropriate to use the weak (with respect to the noise) signal approximation, Eq. (1.20), as we are aiming at the detection of the weakest possible background, which is clearly dominated by the noise.

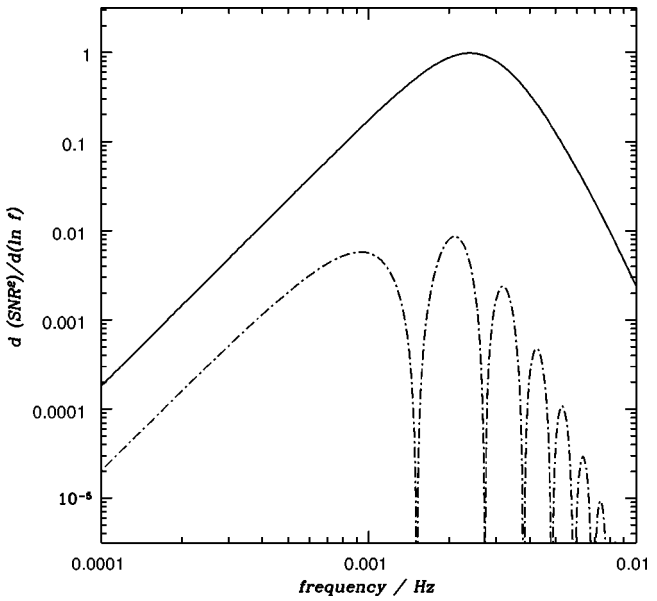

FIG. 4. The contribution of different frequency regions to the total signal-to-noise. The plot shows the fraction of SNR^2, Eq. (1.20), that is accumulated per unit logarithmic frequency interval, $d(\mathrm{SNR}^2)/d(\ln f)$, as a function of the frequency f, for cross-correlations involving a pair of LISA instruments. The vertical axis is normalized so that $\mathrm{SNR}^2=1$ for co-located and co-aligned interferometers, with an arm opening angle of 60°. The solid and dot-dashed lines refer to $D=0$ and $D=1$ AU, respectively. In both cases $\Delta\alpha_0=0$, and the noise spectral density is given by Eq. (2.6).

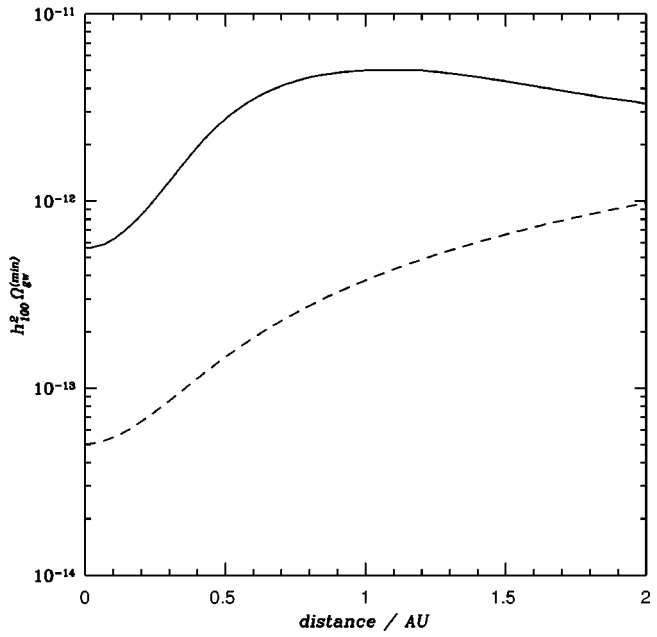

FIG. 5. The minimum detectable value of the fractional energy density of a GW stochastic background. The plot shows $h^2_{100}\Omega^{(\mathrm{min})}$—assumed to be flat [see Eq. (4.1)]—for a cross-correlation experiment involving two identical LISA detectors, as a function of the instrument separation D (in AU). The integration time is set to $T=10^7$ sec. The instrument noise spectral density and the overlap reduction function are given by Eqs. (2.6) and (2.17), respectively; for the sake of simplicity, we set $\Delta\alpha_0=0$ and the integration band corresponds to 10^{-4}–10^{-2} Hz. The dashed line refers to an experiment limited *only by instrumental noise*, where the false alarm probability and the detection rate are 5% and 95%, respectively; in this case $h^2_{100}\Omega^{(\mathrm{min})}$ scales as $T^{-1/2}$. The solid line refers to an experiment limited by *instrumental and confusion noise*, and shows the minimum detectable value of the energy spectrum of a primordial background $h^2_{100}\Omega_p^{(\mathrm{min})}$. In this case, the spectrum of the astrophysical generated background is computed according to Eq. (3.2), and we have optimistically set $\epsilon=0.1$. The limit on $h^2_{100}\Omega_p^{(\mathrm{min})}$ does not improve, in this case, by increasing the integration time and/or lowering the instrumental noise. We refer the reader to the text for further details.

order-of-magnitude range in $h^2_{100}\Omega^{(\mathrm{min})}$ is due to the effect of the overlap reduction function, where the lower limit is for co-located instruments and the upper limit for detectors at a distance D = 2 AU with $\Delta\alpha_0=0$; cf. also Fig. 4.

However, such instrumental sensitivity does not correspond to a comparable sensitivity to PGBs; in fact, the peak of the GGB spectrum, of the order $\sim 10^{-11}$ for the isotropic component, is where the instrument is most sensitive; cf. Fig. 1. In order to quantify this effect and to address the capabilities of space-based interferometers for cosmology, we need a short digression.

Consider a generic two-component stochastic signal

$$\Omega(f)=\Omega_1(f)+\Omega_2(f), \tag{4.2}$$

and assume that $\Omega_1(f)$ and $\Omega_2(f)$ share exactly the same statistical properties (they are isotropic, stationary, Gaussian and unpolarized), and therefore cannot be distinguished from each other. In order to search for $\Omega_1(f)$, one constructs the optimal filter

$$\tilde{Q}_1=\frac{\gamma(f)\Omega_1(f)}{f^3R(f)}, \tag{4.3}$$

and correlates it against the data of two instruments, following the scheme described in the Introduction, Sec. I C. The signal-to-noise ratio at the output of the filtering process is

$$\mathrm{SNR}^2=T\left(\frac{3H_0^2}{10\pi^2}\right)^2\frac{\left(\tilde{Q}_1,\left[\dfrac{\gamma(f)\Omega(f)}{f^3R(f)}\right]\right)^2}{(\tilde{Q}_1,\tilde{Q}_1)}$$
$$=T\left(\frac{3H_0^2}{10\pi^2}\right)^2(\tilde{Q}_1,\tilde{Q}_1)\left\{1+\frac{(\tilde{Q}_1,\tilde{Q}_2)}{(\tilde{Q}_1,\tilde{Q}_1)}\right\}^2. \tag{4.4}$$

The second term in brackets can be interpreted as the (undesired) residual correlation in the detection filter due to $\Omega_2(f)$, which cannot be eliminated. When it exceeds unity, the component Ω_1 cannot be detected, regardless of the instrumental sensitivity; observations carried out with smaller noise disturbances would simply increase both terms $(\tilde{Q}_1,\tilde{Q}_1)$ and $(\tilde{Q}_1,\tilde{Q}_2)$ by exactly the same amount, without improving the chances of detecting Ω_1. The same holds for the integration time T: it has no effect at all on the capability

of discriminating the two components. Therefore, the minimum detectable value of $\Omega_1(f)$ is set by the condition

$$(\tilde{Q}_1,\tilde{Q}_1)=(\tilde{Q}_1,\tilde{Q}_2). \tag{4.5}$$

Notice that the frequency dependence of the two components is very important: if $\Omega_1(f)$ and $\Omega_2(f)$ follow a similar frequency behavior, the filter picks up more power from the ''spurious'' component $\Omega_2(f)$; if they are drastically different, even if $\Omega_2(f)$ dominates $\Omega_1(f)$, one could achieve a detection.

This example describes exactly the issue that we are considering in this section, by simply identifying Ω_1 with Ω_p, and Ω_2 with $\Omega_{g,is}$. The unresolved radiation from binary systems provides therefore a *fundamental sensitivity limit* in searching for the primordial GW background. We have computed this limit from Eq. (4.5) in the case of an experiment carried out with a pair of identical LISA's assuming Ω_p constant and $\Omega_{g,is}(f)$ given by Eq. (3.2). The results are summarized in Fig. 5; the key conclusion is that two LISA detectors will be able to detect a PGB (with constant energy spectrum) only if $h_{100}^2\Omega_p \gtrsim 5\times 10^{-13}$. The big loss of SNR with respect to the case where the experiment is limited only by instrumental noise is due to the fact that the GGB is very strong in the mHz band, and $\Omega_p(f)$ and $\Omega_g(f)$ have a similar decreasing frequency behavior in the frequency window where most of the SNR is accumulated: the residual correlation at the filter output produced by the GGB is large.

Given the results reported in Fig. 5, it is straightforward to conclude that the GGB is a guaranteed, strong GW signal for space-based detectors. In fact, if one constructs a filter matched to a GGB given by Eq. (3.2) and performs cross-correlations between two identical LISA instruments which are characterized by the noise curve (2.6), one can detect such a signal with $\mathrm{SNR_g}\sim 100$, for a time of observation $T=10^7$ sec (see Fig. 6); 2–3 days of integration time are sufficient to reach $\mathrm{SNR_g}\simeq 10$. Two LISA-like detectors would therefore be extremely powerful telescopes to launch deep surveys of populations of binary systems in our Universe with periods between a few hours and a few hundred seconds.

The bottom line of this analysis is therefore clear: *the fundamental limiting factor in searching for a primordial GW background in the* 10^{-5}–10^{-2} Hz *frequency window is the stochastic radiation from unresolved binary systems*. Searches for PGBs with $h_{100}^2\Omega_p \lesssim 5\times 10^{-13}$ thus call for a change in the observational window. We briefly discuss this issue in the next section.

B. Towards testing slow-roll inflation

The mHz frequency window is unsuitable to reach the ambitious sensitivity level $h_{100}^2\Omega_p^{(\mathrm{min})}\sim 10^{-16}$ predicted by slow roll inflation. One needs to design an experiment with optimal sensitivity in a band free from generated backgrounds. Given our present astrophysical understanding, the most promising region seems to be $\sim$0.1–1 Hz, which would be optimally accessible through space-borne interferometers with arms shorter than the LISA ones by a factor of

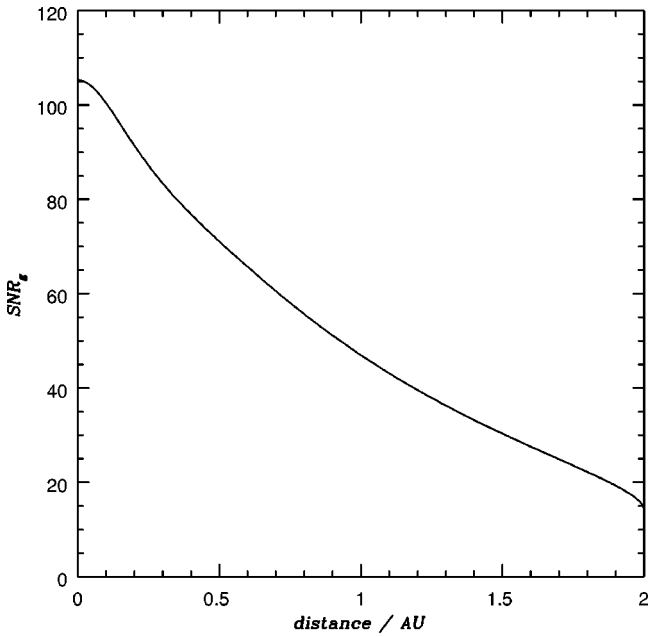

FIG. 6. The signal-to-noise ratio at which the astrophysically generated background can be detected. The plot shows the SNR that can be achieved in 4 months of integration time, correlating the data of a pair of LISA detectors, as a function of the distance D (in AU). The Wiener filter is matched to the signal described by Eq. (3.2).

$\sim$100. In fact, the entire frequency window from $\sim 10^{-7}$ Hz to $\sim$0.1 Hz is contaminated by stochastic signals of astrophysical origin with $h_{100}^2\Omega \gg 10^{-16}$. A background generated by massive black hole binary systems with fractional energy density $h_{100}^2\Omega\sim 10^{-15}$–$10^{-14}$ is present in the μHz range [46]; however, our ignorance concerning the formation rate of massive black holes and the merger rate of massive black hole binary systems in the range $\sim 10^5\ M_\odot$–$10^9\ M_\odot$ prevents us from giving a more solid estimate of the background generated by such objects. For $10^{-5}\ \mathrm{Hz}\lesssim f\lesssim 10^{-2}$ Hz, unevolved binaries and WD-WD binary systems completely swamp the observational window; see Sec. III. Above $\sim$10 mHz the only residual sizable contribution comes from NS-NS binary systems; as we have discussed in Sec. III, above $\sim$0.1 Hz, the number of sources per frequency bin becomes less than 1, and the sky is ''transparent'' to a primordial signal. For rather long integration times $\approx$3 yr, the rms instrumental noise level that is required to test the prediction from slow-roll inflationary models is of the order $\sim 10^{-24}$:

$$h_{100}^2\Omega_p^{(\mathrm{min})}\simeq 8\times 10^{-17}\left(\frac{f}{0.1\ \mathrm{Hz}}\right)^{3/2}\left(\frac{T}{10^8\ \mathrm{sec}}\right)^{-1/2}\left[\frac{h_{\mathrm{rms}}}{10^{-24}}\right]^2. \tag{4.6}$$

Operating at considerably higher frequency than LISA, the two detectors would have to be closely located, $D\lesssim 10^{11}$ cm, in order to have optimal overlap reduction function; however, this also increases potentially correlated noise sources. Clearly the technological challenge to achieve the mentioned sensitivity is considerable; the main noise sources that would

degrade the performance of such a detector are the shot noise, beam pointing fluctuations, and accuracy of the phase measurement technique. This imposes stringent requirements on the power and frequency of the laser, as well as on the dimensions of the ''optics'' and on other components of the instrument. We would also like to stress that the value of $h_{\rm rms}$ that we have quoted in Eq. (4.6) is the *effective* noise fluctuation in the data stream, *after* the spectral lines from individual NS-NS binaries, which are still copiously present in the observation band, have been removed. How this can be effectively done and what instrument sensitivity is required is still an open question that requires a careful analysis [47]. The main result of this crude analysis is that one could indeed reach the target sensitivity, and the fundamental limitations that make the mHz band unsuitable are removed. However, several questions remain open for future analysis: a discussion of these issues goes far beyond the purpose of the present paper.

V. CONCLUSIONS

Gravitational wave experiments in the low-frequency window, together with high-frequency ground-based interferometers, are expected to improve our picture of the very early Universe and the understanding of the behavior of fundamental fields at high energy by detecting or setting stringent upper limits on the primordial background of gravitational radiation.

In this paper we have analyzed the sensitivity of space-borne laser interferometers of the LISA class and possible succeeding missions. In order to set a reference frame for this discussion, we have regarded the detection of a GW background produced during the early Universe of energy $h_{100}^2\Omega_p \sim 10^{-16}$, consistent with the prediction of standard slow-roll inflation, as the goal of GW cosmology. We have assumed the operation of two space detectors, in order to achieve the best sensitivity and detection confidence, and we have shown that the technology available for LISA already ensures the detection of a GW background as weak as $h_{100}^2\Omega \approx 5\times 10^{-14}$. However, the strong stochastic signal in the mHz band due to short-period solar-mass binary systems that cannot be resolved as individual sources prevents us from detecting a primordial background weaker than $h_{100}^2\Omega_p \approx 5\times 10^{-13}$. Astrophysically generated stochastic backgrounds therefore set a fundamental limit in the mHz band that prevents us from achieving a sensitivity that goes beyond what is already guaranteed by the LISA technology. They also represent a guaranteed strong signal detectable at high signal-to-noise ratio, which enables the study of the distribution and merger rate of populations of binary compact objects in the Universe.

Dedicated missions with optimal sensitivity in the window 0.1–1 Hz appear, at present, the only viable option in the search for very weak primordial backgrounds and we have briefly discussed the technological challenges involved in probing slow-roll inflation. Our order-of-magnitude analysis strengthens the hope that a sensitivity level $h_{100}^2\Omega_p \sim 10^{-16}$ might be within the capability of future dedicated low-frequency detectors.

Our analysis clearly indicates the key issues that deserve further investigation: a solid estimate of galactic and extragalactic GW backgrounds produced by astrophysical sources, the investigation of the statistical issues that can lead to the discrimination of the PGB from the GGB, and a more rigorous analysis of the technical and conceptual problems for low-frequency experiments dedicated to GW cosmology. On the observational side, the presently designed single-instrument LISA mission is a fundamental step for the planning of more ambitious, multi-detector experiments: we will be able to measure directly the degree of anisotropy of the generated background, shedding light on the fundamental limiting factor of mHz experiments. In fact, while the present paper deals only with the detection of an isotropic stochastic signal, the remarkable sensitivity of LISA offers the chance of going far beyond: a detailed study of the anisotropy and angular dependence of stochastic signals, both of astrophysical and primordial origin. Such an investigation is currently in progress, and will be reported in a separate publication [48].

ACKNOWLEDGMENTS

We thank C. Cutler and B. Schutz for their help and encouragement throughout this work. We especially thank P. Bender for sharing his latest thoughts on generated stochastic backgrounds and for several comments on a preliminary version of this paper. We would also like to thank K. Danzmann for illuminating discussions regarding LISA technology and the noise sources at low frequencies. This work has also benefited from interactions with B. Falkner and S. Vitale.

APPENDIX

We give here the values of the numerical coefficients that enter expressions (2.14), (2.15) and (2.16) of the overlap reduction function derived in Sec. II B:

$$A_0=\frac{513}{4096},\quad A_1=\frac{135}{1024},\quad A_2=\frac{243}{2048},\quad A_3=-\frac{9}{1024},\quad A_4=\frac{33}{4096}; \tag{A1}$$

$$B_0=-\frac{27\sqrt{3}}{4096},\quad B_1=\frac{27\sqrt{3}}{1024},\quad B_2=-\frac{81\sqrt{3}}{2048},\quad B_3=\frac{27\sqrt{3}}{1024},\quad B_4=-\frac{27\sqrt{3}}{4096}; \tag{A2}$$

$$C_0=\frac{513}{8192},\quad C_1=\frac{171}{2048},\quad C_2=\frac{99}{4096},\quad C_3=\frac{27}{2048},\quad C_4=\frac{33}{8192}; \tag{A3}$$

$$D_0=-\frac{27\sqrt{3}}{8192},\quad D_1=-\frac{9\sqrt{3}}{2048},\quad D_2=\frac{63\sqrt{3}}{4096}, \tag{A4}$$

$$D_3=-\frac{9\sqrt{3}}{2048},\quad D_4=-\frac{27\sqrt{3}}{8192};$$

$$E_0=\frac{513}{16384},\quad E_1=\frac{207}{4096},\quad E_2=\frac{339}{8192},$$

$$E_3=\frac{63}{4096},\quad E_4=\frac{33}{16384};\tag{A5}$$

$$F_0=-\frac{27\sqrt{3}}{16384},\quad F_1=-\frac{45\sqrt{3}}{4096},$$

$$F_2=-\frac{177\sqrt{3}}{8192},\tag{A6}$$

$$F_3=-\frac{45\sqrt{3}}{4096},\quad F_4=-\frac{27\sqrt{3}}{16384}.$$

[1] M. Maggiore, Phys. Rep. **331**, 28 (2000).
[2] T. Creighton, ''Gravitational waves and the cosmological equation of state,'' gr-qc/9907045.
[3] P. L. Bender *et al.*, ''LISA Pre-Phase A Report,'' 2nd ed., Report No. MPQ 233, 1998; P. L. Bender *et al.*, ''LISA: Laser Interferometer Space Antenna. A Cornerstone Mission for the Observation of Gravitational Waves,'' System and Technology Study Report No. ESA-SCI(2000)11, 2000; available at ftp://ftp.rzg.mpg.de/pub/grav/lisa/sts-1.04.pdf
[4] C. L. Bennett *et al.*, Astrophys. J. Lett. **464**, L1 (1996).
[5] V. Kaspi, J. Taylor, and M. Ryba, Astrophys. J. **428**, 713 (1994).
[6] E. W. Kolb and M. Turner, *The Early Universe* (Addison-Wesley, Redwood City, CA, 1990).
[7] L. Grishchuk, Class. Quantum Grav. **10**, 2449 (1993).
[8] L. Krauss and M. White, Phys. Rev. Lett. **69**, 869 (1992).
[9] M. Turner, Phys. Rev. D **55**, 435 (1997).
[10] G. Veneziano, Phys. Lett. B **265**, 287 (1991).
[11] M. Gasperini and G. Veneziano, Astropart. Phys. **1**, 317 (1993).
[12] M. Gasperini and G. Veneziano, Mod. Phys. Lett. A **8**, 3701 (1993).
[13] R. Brustein, M. Gasperini, M. Giovannini, and G. Veneziano, Phys. Lett. B **361**, 45 (1995).
[14] R. Brustein, M. Gasperini, and G. Veneziano, Phys. Rev. D **55**, 3882 (1997).
[15] A. Buonanno, M. Maggiore, and C. Ungarelli, Phys. Rev. D **55**, 3330 (1997).
[16] B. Allen and R. Brustein, Phys. Rev. D **55**, 3260 (1997).
[17] C. Ungarelli and A. Vecchio, in *Gravitational Waves*, edited by S. Meshkov, AIP Conf. Proc. No. 523 (AIP, Melville, NY, 2000).
[18] M. S. Turner and F. Wilczek, Phys. Rev. Lett. **65**, 3080 (1990).
[19] M. Kamionkowski, A. Kosowsky, and M. S. Turner, Phys. Rev. D **49**, 2837 (1994).
[20] A. Riotto and M. Trodden, Annu. Rev. Nucl. Part. Sci. **49**, 35 (1999).
[21] M. Carena, M. Quirós and C. Wagner, Phys. Lett. B **380**, 81 (1996).
[22] M. Carena, M. Quirós, and C. Wagner, Nucl. Phys. **B524**, 3 (1998).
[23] M. Laine and K. Rummukainen, Phys. Rev. Lett. **80**, 5259 (1998).
[24] R. A. Battye, R. R. Caldwell, and E. P. S. Shellard, in ''Topological Defects in Cosmology,'' edited by F. Melchiorri and M. Signore, 1997, astro-ph/9706013.
[25] L. Krauss, Phys. Lett. B **284**, 229 (1992).
[26] C. J. Hogan, in *Laser Interferometer Space Antenna*, edited by W. M. Falkner, AIP Conf. Proc. No. 456 (AIP, Woodbury, NY, 1998), pp. 79–86.
[27] C. J. Hogan, Phys. Rev. Lett. **85**, 2044 (2000).
[28] E. Flanagan, Phys. Rev. D **48**, 2389 (1993).
[29] B. Allen and J. D. Romano, Phys. Rev. D **59**, 102001 (1999).
[30] C. Cutler, Phys. Rev. D **57**, 7089 (1998).
[31] D. Hils, P. L. Bender, and R. F. Webbink, Astrophys. J. **360**, 75 (1990).
[32] P. L. Bender and D. Hils, Class. Quantum Grav. **14**, 1439 (1997).
[33] K. A. Postnov and M. E. Prokhorov, Astrophys. J. **494**, 674 (1998).
[34] D. I. Kosenko and K. A. Postnov, Astron. Astrophys. **336**, 786 (1998).
[35] R. Schneider, V. Ferrari, S. Matarrese, and S. F. Portegies Zwart, ''Gravitational Waves From Cosmological Compact Binaries,'' astro-ph/0002055.
[36] D. I. Kosenko and K. A. Postnov, Astron. Astrophys. **355**, 1209 (2000).
[37] G. Giampieri and A. G. Polnarev, Mon. Not. R. Astron. Soc. **291**, 149 (1997).
[38] R. F. Webbink, Astrophys. J. **277**, 355 (1984).
[39] P. Madau, H. C. Ferguson, and M. Dickinson, Mon. Not. R. Astron. Soc. **283**, 1388 (1996).
[40] P. Madau, L. Pozzetti, and M. Dickinson, Astrophys. J. **498**, 106 (1997).
[41] E. S. Phinney, Astrophys. J. Lett. **380**, L17 (1991).
[42] R. Narayan, T. Piran, and A. Shemi, Astrophys. J. Lett. **379**, L17 (1991).
[43] V. Kalogera, R. Narayan, D. N. Spergel, and J. H. Taylor, ''The Coalescence Rate of Double Neutron Stars Systems,'' astro-ph/0012038.
[44] M. Tinto, J. W. Armstrong, and F. B. Estabrook, Phys. Rev. D **63**, 021101 (2001).
[45] B. F. Schutz, talk given at the Third LISA Symposium.
[46] M. Rajagopal and R. W. Romani, Astrophys. J. **446**, 543 (1995).
[47] R. Stebbins, talk given at the Third LISA Symposium [45].
[48] C. Ungarelli and A. Vecchio (in progress).